

Research Article

Open Access



# Flexible and breathable MXene-modified paper-based piezoresistive pressure sensors integrated into airbag pillow for sleep monitoring

Yanxi Zhang<sup>1</sup>, Baojia Zhang<sup>1</sup>, Yu Lv<sup>1</sup>, Peng Wang<sup>2\*</sup>, Teng Liu<sup>1\*</sup>, Chuizhou Meng<sup>1\*</sup>

<sup>1</sup>State Key Laboratory for Reliability and Intelligence of Electrical Equipment, Engineering Research Center of Ministry of Education for Intelligent Rehabilitation Device and Detection Technology, Hebei Key Laboratory of Smart Sensing and Human-Robot Interaction, School of Mechanical Engineering, Hebei University of Technology, Tianjin 300401, China.

<sup>2</sup>School of Mechanical Engineering, University of Jinan, Jinan 250022, Shandong, China.

\***Correspondence to:** Dr. Peng Wang, School of Mechanical Engineering, University of Jinan, 336 Nanxinzhuan West Road, Shizhong District, Jinan 250022, Shandong, China. E-mail: wangp0405@163.com; Prof. Teng Liu, Prof. Chuizhou Meng, State Key Laboratory for Reliability and Intelligence of Electrical Equipment, Engineering Research Center of Ministry of Education for Intelligent Rehabilitation Device and Detection Technology, Hebei Key Laboratory of Smart Sensing and Human-Robot Interaction, School of Mechanical Engineering, Hebei University of Technology, 5340 Xiping Road, Beichen District, Tianjin 300401, China. E-mail: wuqiu-liu@163.com; 2018108@hebut.edu.cn

**How to cite this article:** Zhang, Y.; Zhang, B.; Lv, Y.; Wang, P.; Liu, T.; Meng, C. Flexible and breathable MXene-modified paper-based piezoresistive pressure sensors integrated into airbag pillow for sleep monitoring. *Soft Sci.* 2025, 5, 17. <https://dx.doi.org/10.20517/ss.2024.68>

**Received:** 30 Nov 2024 **First Decision:** 30 Dec 2024 **Revised:** 13 Feb 2025 **Accepted:** 19 Feb 2025 **Published:** 14 Mar 2025

**Academic Editors:** YongAn Huang, Toan Dinh **Copy Editor:** Pei-Yun Wang **Production Editor:** Pei-Yun Wang

## Abstract

Sleeping head monitoring through an intelligent pillow is crucial in warning of disastrous diseases such as suffocation during snoring. However, flexible sensors are still inferior due to limited sensing performance and impermeable wearing discomfort. Herein we develop a flexible pressure sensor by constructing both decorated MXene piezoresistive network and printed interdigital silver electrodes on a dust-free paper platform. The intrinsic paper fabric framework provides good permeability for comfortable skin-attaching, and the microstructured MXene on paper offers good sensing performance with high sensitivity ( $16.7 \text{ kPa}^{-1} < 20 \text{ kPa}$ ), a wide detection range ( $\sim 100 \text{ kPa}$ ), and fast response time ( $\sim 50 \text{ ms}$ ). As a proof of concept, the single sensor unit integrated into an airbag pillow for different types of snoring monitoring and five sensor arrays for sleeping head posture recognition by machine learning are both demonstrated. The proposed paper-based sensor, along with the intelligent airbag pillow, provides a promising approach for sleep monitoring in a comfortable unrestricted way.

**Keywords:** Flexible and breathable sensor, piezoresistive pressure sensor, MXene, paper, snoring monitoring, sleep monitoring



© The Author(s) 2025. **Open Access** This article is licensed under a Creative Commons Attribution 4.0 International License (<https://creativecommons.org/licenses/by/4.0/>), which permits unrestricted use, sharing, adaptation, distribution and reproduction in any medium or format, for any purpose, even commercially, as long as you give appropriate credit to the original author(s) and the source, provide a link to the Creative Commons license, and indicate if changes were made.



## INTRODUCTION

It is known that sleep accounts for one-third of a person's life and the quality of sleep plays a crucial role in restoring the person's health status. For patients with sleeping diseases such as suffocation during snoring, convenient and efficient sleep monitoring ways are necessary for warning of potential risks. However, traditional sleep monitoring tools such as polysomnography (PSG) and portable devices must be used with complex wires connected to bulky equipment, severely limiting their popularized application in daily life. In comparison, wearable sensors capable of acquiring physiological signals and posture information have become an alternative way for sleep monitoring<sup>[1]</sup>. However, they need to be tightly worn on the human body, which still interferes with the quiet sleeping experience. Therefore, it is of significance to develop an effective approach to monitoring the sleep status in an unrestricted way, and the intelligent pillow integrated with flexible sensors that can monitor the health status of the sleeper through their contact with the sleeper's head would meet such need.

Flexible pressure sensors<sup>[2,3]</sup>, as key components of wearable electronics, have attracted great attention for their applications in the fields of human health monitoring<sup>[4,5]</sup>, electronic skin<sup>[6,7]</sup>, and human-machine intelligence<sup>[8]</sup>. Among various pressure sensing mechanisms such as piezoresistive<sup>[9]</sup>, capacitive<sup>[10,11]</sup>, and piezoelectric<sup>[12]</sup> ones, capable of converting pressure stimuli into responding resistive signals, have been widely studied because of their simple device configuration, easy signal acquisition, and low cost. Though progress has been made, piezoresistive pressure sensors with high sensitivity, wide detection range, fast response, and stable reliability are still under pursuit. Recently, the microstructuring strategy has been proven to be an effective way to improve sensitivity, and the typical microstructures include a pyramid<sup>[13,14]</sup>, a dome<sup>[15,16]</sup>, and so on. However, typically expensive equipment and complex microfabrication processes are needed to construct such regular microstructures, which limits their mass production and vast application. Therefore, it is still a challenge to fabricate flexible performance-enhanced pressure sensors in a facile and economical way<sup>[17]</sup>. Meanwhile, current flexible sensors are designed and fabricated on impermeable polymer film substrates, which would cause itching of the skin after a long time covering of the skin<sup>[18-20]</sup>. Therefore, for flexible sensors to be integrated into pillows that will contact the sleeper's head during the whole night, breathability becomes a highly required merit for a comfortable sleeping experience.

In this work, we report the design and fabrication of a flexible pressure sensor by constructing both the decorated MXene piezoresistive network and the printed interdigital silver electrodes on a dust-free paper platform. The intrinsic fabric of the paper provides good permeability for comfortable skin-attaching, and the microstructured MXene on fabric offers high sensing performance with high sensitivity ( $16.7 \text{ kPa}^{-1} < 20 \text{ kPa}$ ), a wide detection range ( $\sim 100 \text{ kPa}$ ), and fast response time ( $\sim 50 \text{ ms}$ ). As a proof of concept, the developed sensors integrated into an airbag pillow for snoring monitoring and sleeping head posture recognition are well demonstrated. The proposed paper-based sensor, along with the intelligent airbag pillow, provides a promising approach for sleep monitoring in a comfortable unrestricted way.

## EXPERIMENTAL

### Materials

Dust-free paper (Saige, Kunshan, China) was used as the fabric substrate for MXene sheet coating and silver electrode printing. Silver paste (Mifang, Shanghai, China) was used to print the interdigital electrodes. Conductive tape (Deyi, Guangzhou, China) was used to connect sensors and devices.

### Preparation of MXene

The hydrochloric acid etching method was used to prepare MXene, in which the Al layer elements in the MAX phase were selectively etched by dilute hydrochloric acid. The typical procedure is as follows: 7.5 mL

of concentrated hydrochloric acid was added to 2.5 mL of deionized water, and then 0.8 g of lithium fluoride was added, followed by stirring the mixture at 400 rpm for 5 min at room temperature. Afterward, 0.5 g of  $\text{Ti}_3\text{AlC}_2$  was added with stirring at 500 rpm at 47 °C for 24 h, and then deionized water was added, followed by centrifuging the mixture seven to eight times. Finally, the mixture dispense was treated by ultrasonic and centrifugation at 3,000 rpm for 20 min, and the supernatant was MXene.

### Preparation of the sensor

The prepared MXene was dropped in deionized water, followed by stirring for 20 min and ultrasonic for 5 min to obtain the well-dispersed diluted MXene solution. Then the prepared MXene solution was poured into a shallow container, and a piece of dust-free paper was laid flat on the surface of the solution. Because of the hydrophilic nature of the paper fibers, the paper would adsorb the water into its fabric network and sink with immersion in the solution. MXene can be firmly attached on the surface of fibers due to the interaction of functional groups, forming a MXene coating layer on the fabric framework. The dip-coating process lasts for 10 s each time, followed by vacuum drying at 40 °C to further anchor the coating of MXene on fibers. Multiple cycles of dip-coating and vacuum drying can be applied to coat more MXene on the dust-free paper to finally obtain the piezoresistive layer. The interdigital electrodes were made by screen printing silver paste on another piece of dust-free paper to obtain the electrode layer. The screen plate has a mesh size of 250, a wire diameter of 40  $\mu\text{m}$ , and a screen thickness of 68  $\mu\text{m}$ . The piezoresistive layer and the electrode layer were compressed together with sides taped to obtain the sensor unit.

### Characterization and measurements

The morphology of the prepared fabric samples was characterized by a high-resolution field-emission scanning electron microscopy (HRFE SEM, JEOL 7610F, Japan Electronics Co., Ltd.), with energy dispersive spectroscopy (EDS) for the elemental distribution analysis. The sensor was placed on a flat heating table with adjustable temperature (2020, Shenzhen Hualianchuang Electronic Tools Co., Ltd) to test the effect of temperature on it. The associated resistance was measured with a high-precision LCR meter (6300, Guwei Electronic Industry Co., Ltd.). A pressure load is applied by a high-precision universal testing machine (HTS-LLY9120B, Guangdong Zhongye Instrument Equipment Co., Ltd.) to test the sensing performance. For the biocompatibility test on human skin, the sensor and poly(dimethylsiloxane) (PDMS) film were tightly attached to the skin of the volunteer's forearm for ten days, and the color and health state of the covered skin were observed.

## RESULTS AND DISCUSSION

### Design, fabrication and application of the sensor

For simplicity of the device configuration, the sensor adopts a concise two-layered structure by compressing an MXene network-based piezoresistive layer on top of an interdigital silver electrode layer, both of which are constructed on the dust-free paper substrates. Being an emerging two-dimensional (2D) material with excellent electrical conductivity and high specific surface area, MXene has been proven to be an effective sensitive material with nano-/micro-structures for improved sensing performance for flexible sensors<sup>[21,22]</sup>. MXene is obtained by the hydrochloric acid-etching method in an aqueous solution [Figure 1A], and the scanning electronic microscopy (SEM) image shows the typical accordion-like layer structure of  $\text{Ti}_3\text{C}_2\text{T}_x$  powder [Figure 1B], which facilitates the formation of MXene network in the paper fabric. The hydrophilic groups in the aqueous solution of MXene interact with the hydrophilic groups in the paper fibers through the hydrogen bonding and capillary action effects, prompting the deposition of MXene flakes on the surface of the paper fibers and the formation of a stable conductive network through functional groups bonding. After being picked up and vacuum-dried, the dust-free paper decorated with MXene network can be used as the piezoresistive layer [Figure 1C, bottom line]. The interdigital silver electrodes are printed on another piece of dust-free paper using the screen-printing technique [Figure 1C, upper line]. In the end, the

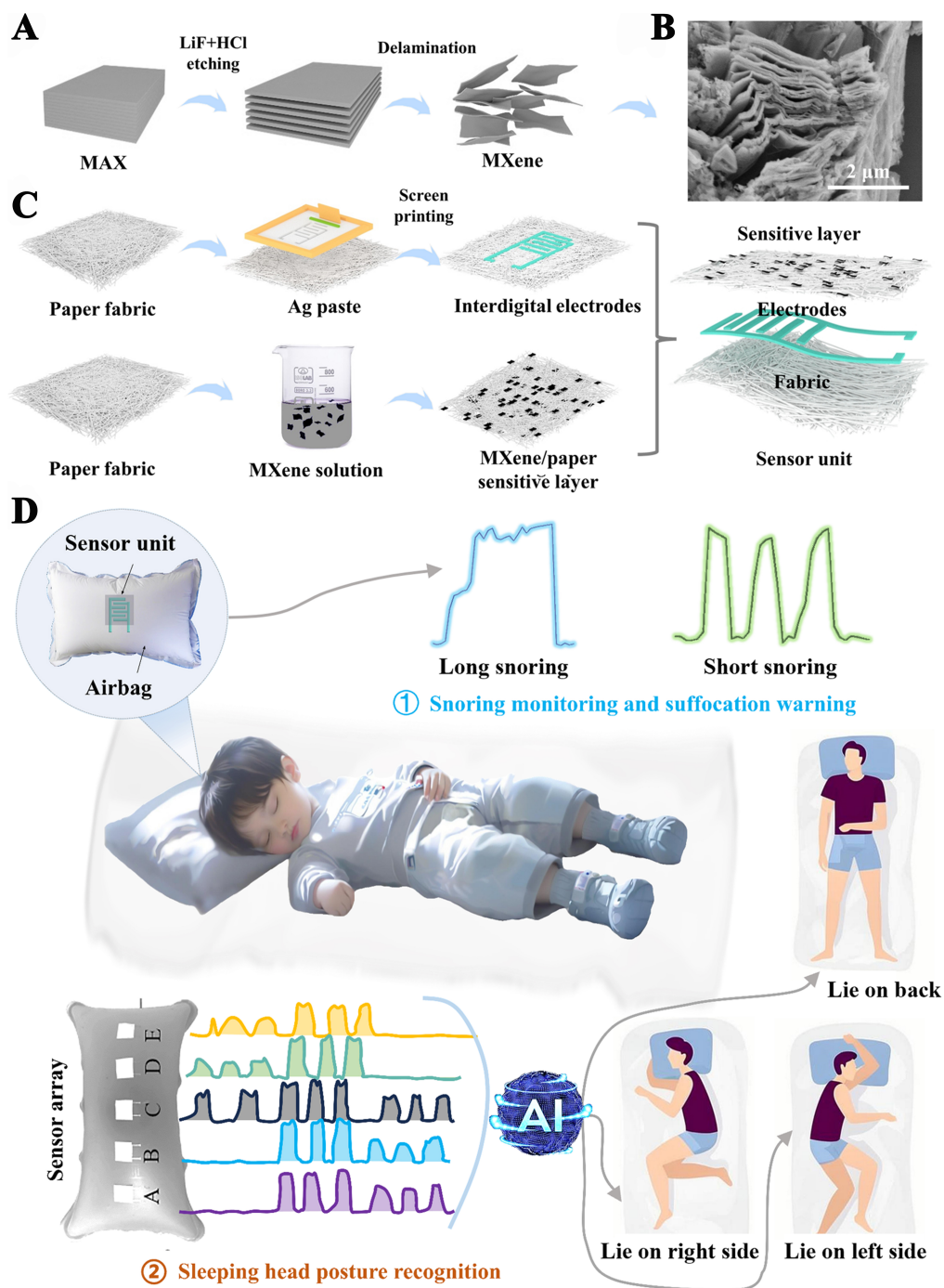


**Figure 1.** Design, fabrication and application of the sensor. (A) Schematic diagram illustrating the preparation of MXene by the hydrochloric acid-etching method; (B) SEM image of the MXene sheets; (C) Schematic diagram illustrating the fabrication of the MXene-based piezoresistive layer and the interdigital silver electrodes on dust-free paper and the assembly of the sensor unit; (D) Schematic diagram illustrating the sensor unit integrated into the airbag pillow for snoring monitoring and the sensor array for head posture recognition by machine learning. SEM: Scanning electronic microscopy.

prepared sensitive layer is compressed on top of the electrode layer to obtain the single sensor unit [Figure 1C, right part].

Due to the flexibility and breathability, the designed pressure sensors can be integrated into an airbag pillow for long-term snoring monitoring and sleeping head posture recognition with skin-attaching comfort [Figure 1D].

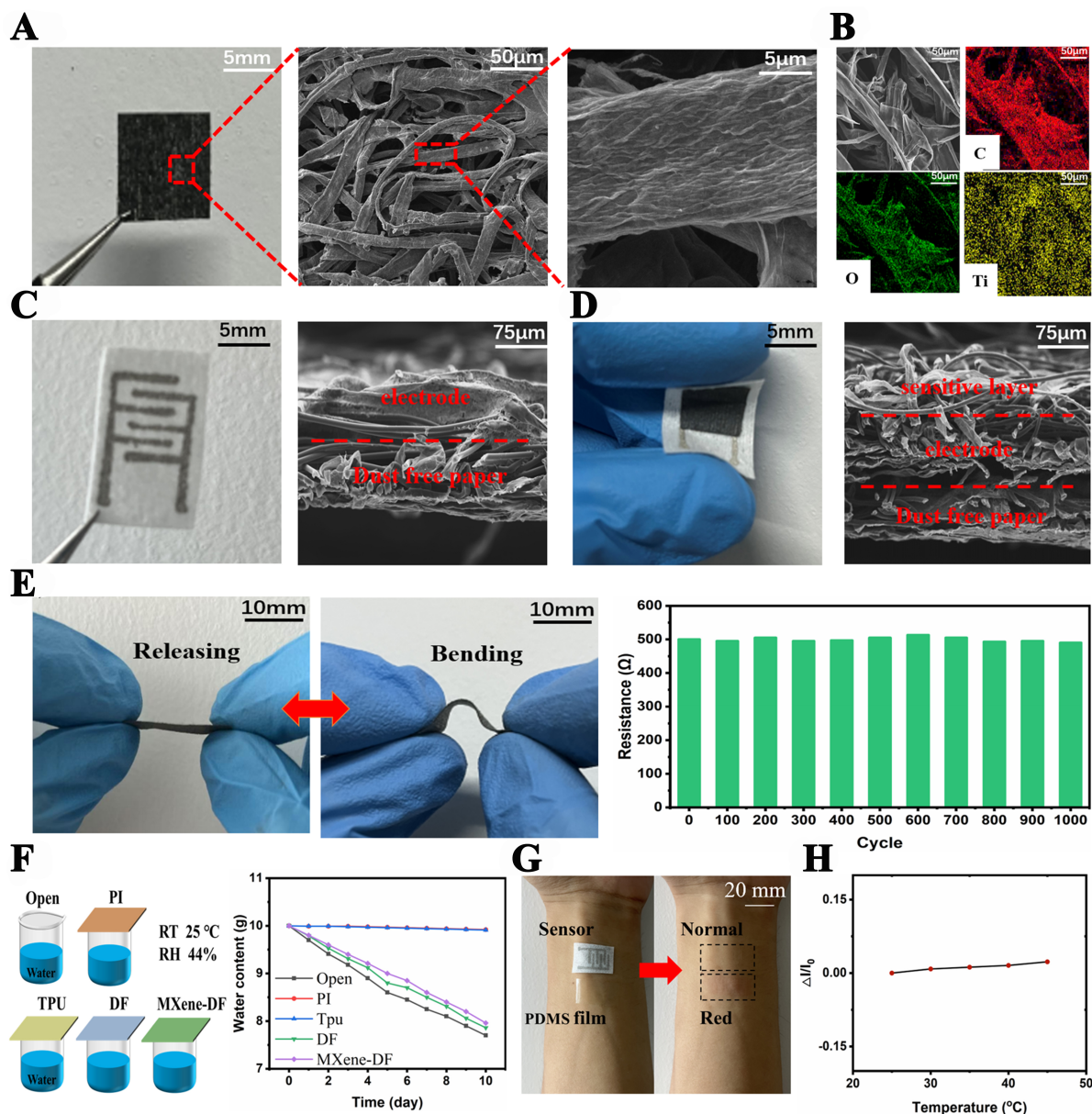
### Characterization and measurements of the sensor

Figure 2A shows the photograph of the prepared MXene/dust-free paper with black color, indicating the successful incorporation of MXene on the paper substrate. SEM images further reveal that the MXene sheets form a tight and wrinkled coating layer around the fibers in the paper. Element mapping images present that the major elements of C, O, and Ti are uniformly distributed, indicating the uniform coating of MXene [Figure 2B]. Figure 2C clearly shows the photograph of the printed interdigital silver electrodes on the dust-free paper. SEM images further reveal that the solid silver paste is deposited on the fabric framework to form the continuous electrode from a cross-sectional view [Figure 2C]. To make a complete sensor, the size of the sensitive layer is 12 mm × 12 mm, which is large enough to cover the effective interdigital electrode led region of 10 mm × 10 mm, and the designed interdigital electrodes [Supplementary Figure 1] are printed on a dust-free paper with a size of 20 mm × 15 mm as the substrate. The thickness of the sensitive layer is around 0.25 mm and the overall thickness of the assembled sensor unit is around 0.8 mm. Figure 2D shows that the sensor unit can be bent as one integrated unit due to the use of a paper fabric framework as substrate, and its layered structure can be seen from the SEM cross-sectional view with element mapping [Supplementary Figure 2]. It is noted that the gap between the sensitive layer and the electrode layer facilitates loose contact between the two, leading to a small initial current and then a large relative current change for a large sensitivity. The edges of the sensitive layer and the electrode layer are bonded with adhesive glue, so the assembled sensor is an integrated unit. It will not delaminate during practical bending usage.

After being coated with MXene, the dust-free paper shows a moderate conductivity of 16 S·m<sup>-1</sup> to serve as a sensitive layer. In addition, its mechanical property is also enhanced due to the bonding effect between the MXene and the paper fibers [Supplementary Figure 3]. Its resistance is measured to be changed a little (within 2.4%) after being bent with a bending radius of 2 mm 1,000 times [Figure 2E], indicating its consistently stable resistance for frequently flexible usage. To demonstrate the breathability of the paper-based sensor, the sensor and different comparing sample films are used to cover a beaker filled with water at the same room temperature with 44% humidity for days and the remaining water content is measured [Figure 2F]. The opened beaker has the largest water-losing rate, which is the most air and moisture-free-moving case. The pristine dust-free paper has the second largest water-losing rate, indicating the breathability of the paper due to its intrinsic fabric pores. After decorating MXene, the dust-free paper still offers a similar large water-losing rate as the pristine one, indicating that good breathability is well reserved. In contrast, the beaker covered with impermeable polyimide (PI) and thermoplastic polyurethane (TPU) films (widely used conventional polymer substrates for developing flexible electronics) offers almost no water loss. Due to the breathability of the paper-based sensor, the skin covered by it for ten days remains the healthy status while the one covered by the impermeable PDMS film becomes itching with redness [Figure 2G]. The influence of environmental temperature on the sensor is evaluated, and it is found that the resistance keeps a very slow increase as the temperature increases from 20 to 45 °C [Figure 2H], indicating the sensor is capable of delivering relatively stable sensing performance without significant drifting when used in the body temperature range. In addition, the environmental humidity also has little impact on the sensor [Supplementary Figure 4].

### Sensing performance of the sensor

The sensor adopts the piezoresistive pressure sensing mechanism for a simplified device structure. Different from conventional piezoresistive sensors with two electrodes sandwiching one sensitive layer, the sensor



**Figure 2.** Characterization and measurements of the sensor. (A) Photograph and SEM images of the MXene/dust-free paper-sensitive layer; (B) Elemental mapping of C, O, and Ti in the sensitive layer; (C) Photograph of the interdigital silver electrode layer and SEM image showing the cross-sectional view; (D) Photograph of the assembled paper-based sensor and SEM images showing the cross-sectional view; (E) Measurement of the resistance of the sensitive layer after 1,000 bending cycles; (F) Measurement of breathability between the paper-based sensor and other films; (G) Photographs showing the skin status after being covered by the paper-based sensor and PDMS film for 10 days; (H) Influence of temperature on the sensor. SEM: Scanning electronic microscopy; PDMS: poly(dimethylsiloxane).

utilizes the novel planar configuration by placing the MXene/dust-free paper sensitive layer on top of the printed interdigital silver electrodes, which yields a more compact structure for its further integration with airbag pillow [Figure 3A]. The corresponding equivalent circuit is drawn connecting one changeable resistor ( $R$ , internal resistance of the sensitive layer) with two changeable resistors ( $R_{\pm}$ , contact resistance between the sensitive layer and the two electrodes). When subjected to an external force, the MXene-based fabric network is compressed with MXene sheets closer to each other, leading to a more conductive pathway

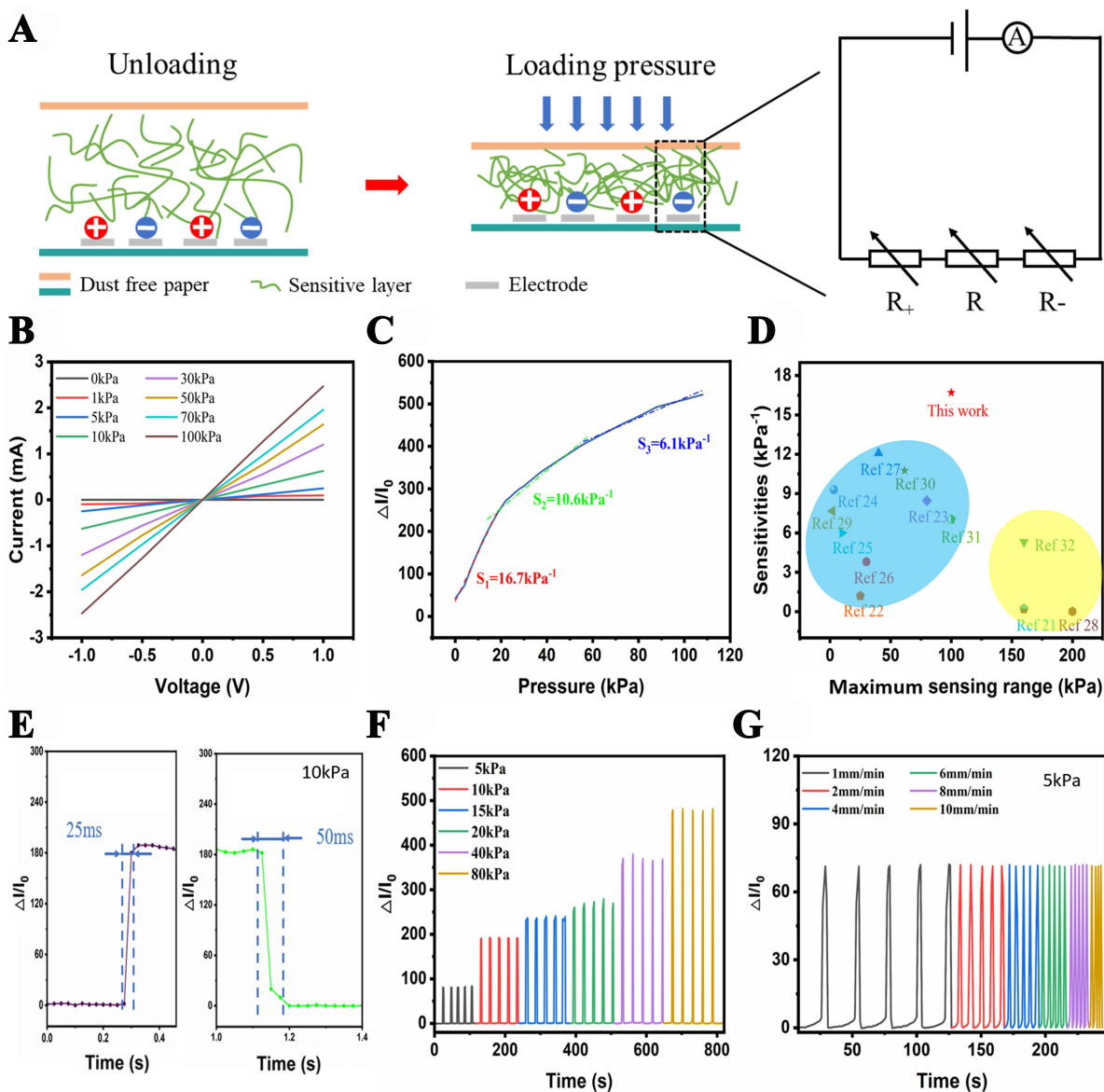


**Figure 3.** Sensing performance of the sensor. (A) Schematic diagram illustrating the conductive MXene-based fabric piezoresistive sensing mechanism and corresponding equivalent circuit; (B) I-V curves under different pressures; (C) Relative current change curve upon pressure; (D) Comparison of the sensitivity and detection range between our sensor and previously reported ones; (E) Response and recovery time. Dynamic behavior (F) under escalating pressures and (G) different frequencies.

and thus decreased internal resistance. Meanwhile, the effective contact area between the sensitive layer and the two electrodes also correspondingly increases upon the applied pressure, causing the contact resistances to decrease. Compared with a conventional solid sensitive layer with no internal microstructures, the highly porous structure of the sensitive layer can provide a prominent resistance change during the compression process. Additionally, the loose contacting state between the porous sensitive layer and the electrodes ensures a very small initial resistance value with no pressure applied. Therefore, the relative resistance change value by dividing the resistance change with the initial resistance is huge, facilitating the achievement of a very high sensitivity.

In practice, the sensitivity ( $S$ ) is measured as  $S = (\Delta I/I_0)/\Delta P$  where  $\Delta I$  is the relative current change with pressure,  $I_0$  is the current at no pressure, and  $\Delta P$  is the applied pressure. [Figure 3B](#) shows the I-V curves with good linear characteristics over up to 100 kPa, indicating a stable piezoresistive response and the ability to discriminate different pressures over a wide detection range. [Figure 3C](#) plots the sensitivity curve across the whole detection range, which mainly consists of three linear regions:  $16.7 \text{ kPa}^{-1}$  within 0-20 kPa,  $10.6 \text{ kPa}^{-1}$  within 20-40 kPa, and  $6.1 \text{ kPa}^{-1}$  within 40-100 kPa. The explanation can be described as follows: in the first linear region, without compression, the porous space between paper fibers is very large. Upon initial compression, the deformation of the porous network is prominent, starting to get MXene connected with formation of many conductive contacting points. Therefore, a small force can induce a large resistance reduction, leading to a large sensitivity. In the second linear region, as compression continues, the conducting pathways formed by MXene connection tend to saturate. Further compression would cause the porous network to further deform with paper fibers to contact each other. The network tends to become compact and the resistance reduces at a slower rate, leading to a medium sensitivity. In the third linear region, after all the voids are closed, further compression would shorten the thickness of the compact MXene/paper fiber solid sheet. The resistance can be further reduced but at a very slow rate, leading to a small sensitivity. The influence of MXene dip-coating cycles on the sensitivity was also evaluated. As the dip-coating time increases, the sensitivity correspondingly increases [[Supplementary Figure 5](#)], because decoration of more MXene leads to more conductive pathing ways in the network. [Figure 3D](#) comprehensively compares our sensor with previously reported paper-based pressure sensors in the aspect of sensitivity and detection range<sup>[22-32]</sup>, showing our sensor yields the best sensing performance. Due to the readily availability and simplicity of fabrication, our sensor can meet the industrial and commercial mass production requirements. [Figure 3E](#) measures the response and recovery times to be  $\sim 25$  and  $45 \sim$  ms, respectively, by taking the average value of five consecutive waveforms [[Supplementary Figure 6](#)], which indicates the quick detection capability for real-time monitoring. [Figure 3F](#) shows good dynamic behavior under escalating pressures and different frequencies with distinct and consistent response peaking curves, ensuring its ability to detect different physiological signals and body motions in a fast and accurate way. [Figure 3G](#) shows the cyclic pressure detection under different compression rates from slow ( $\sim 1 \text{ mm}\cdot\text{min}^{-1}$ ) to fast ( $\sim 10 \text{ mm}\cdot\text{min}^{-1}$ ) by the same 5 kPa, which demonstrates a stable dynamic sensing behavior. The long-term stability is also verified by repeatedly loading and unloading a pressure for 10,000 cycles, and stable response curves with no drifting are observed [[Supplementary Figure 7](#)].

#### Application of sensor unit on airbag pillow for snoring monitoring

Due to the good breathability and excellent sensing performance, the flexible sensor can be worn on different parts of the human body to detect various human activities such as finger bending, hand gripping, throat swallowing, mouth breathing, and wrist pulse beating [[Supplementary Figure 7](#)]. Especially the can sensor can be used to detect joint bending for posture and gesture monitoring. During practical wearable usage, because the sensor is assembled by multiple layers, severe tearing with excessive sheering force should be prohibited to avoid delamination. In addition to being attached to the human body, the developed flexible and breathable sensor can also be integrated into an airbag pillow for sleep monitoring [[Figure 4A](#)], with detection of the airbag internal pressure using a home-built signal acquisition and processing system [[Figure 4B](#)]. The relative current of the sensor and the internal pressure of the airbag can be simultaneously acquired [[Figure 4C](#)], which is used as a reference for subsequent experiments.

[Figure 4D](#) shows that the activities of lying down and sitting up can be detected through the jumping and dropping of the response waveform due to contacting of the head with the sensor. Besides, when lying down, the activity of snoring can also be detected because it applies more pressure on the sensor during snoring. Furthermore, the amplitude and duration of the snoring waveform can be used to distinguish different snoring modes. The explanation can be described as follows: after lying down on the bed, the back

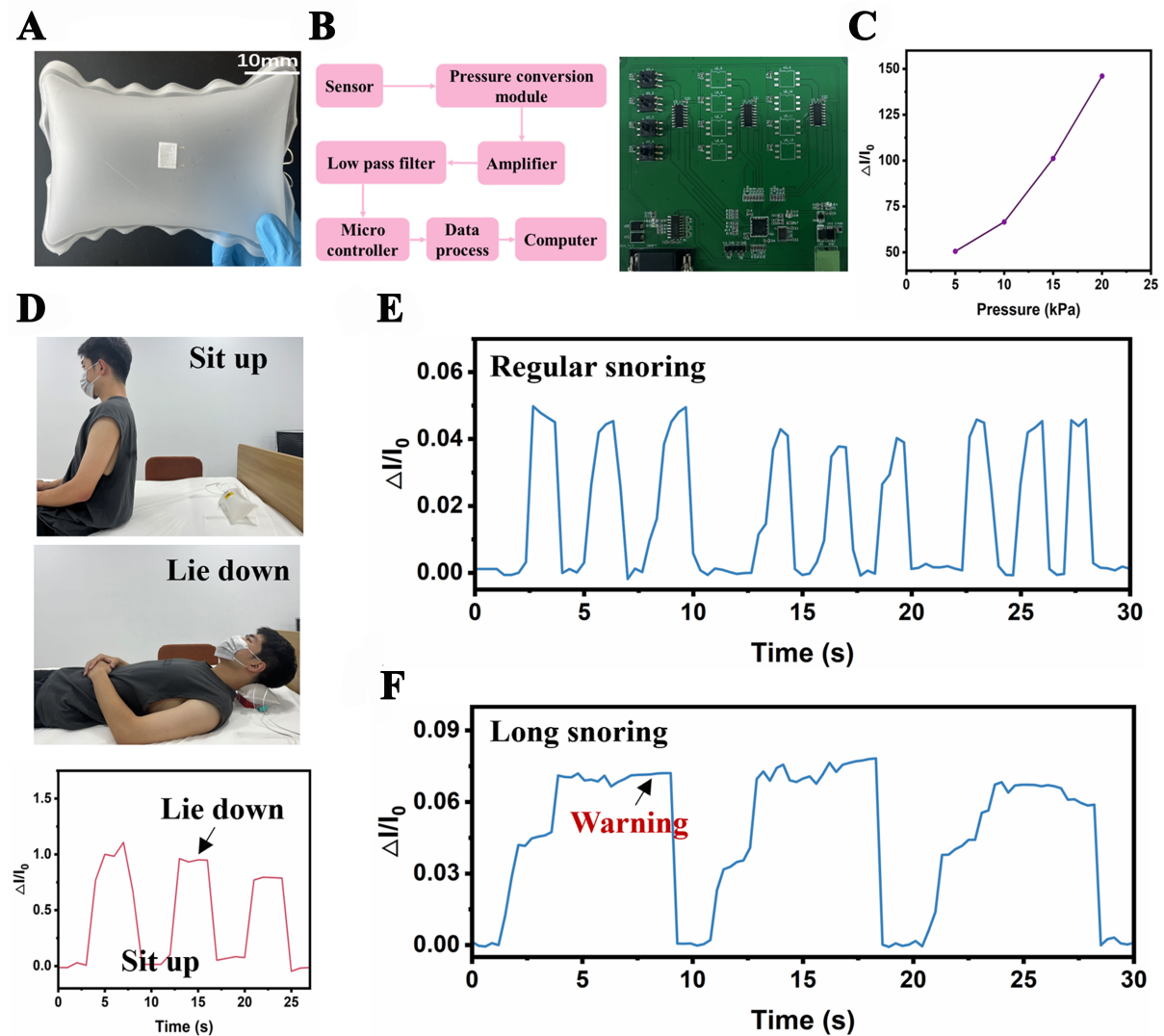


**Figure 4.** Integration of sensor unit on airbag pillow for snoring monitoring. (A) Photograph showing one single sensor unit mounted on the top layer of one airbag; (B) Flowchart illustrating the acquired signal processing process and a photograph showing the home-made circuit board of the electromechanical system; (C) Relative current change curve upon different internal pressures of the airbag; (D) Photograph showing the lie-down and sit activities and corresponding response signals. Comparison of response signals obtained from different snoring modes of (E) normal regular snoring and (F) abnormal long snoring.

of the head and the neck would rest on the airbag pillow. The snoring happens during the strong inhalation stage. In order to open the throat wider to inhale air, the chest expands and the mouth moves upward with the back of the head and the neck further pressing down the airbag pillow, leading to a rising response pressure curve detected by the sensors. In addition, the height of the waveform is positively correlated with the strength of the snoring, and the length is positively correlated with the duration of the snoring. Therefore, the status of the snoring can be deduced from the characteristics of the waveforms. Figure 4E shows that a normal snoring mode yields a regular snoring period of around 2 s with a resting period of around 2 s, while abnormal snoring mode outputs long-duration snoring with almost 5 s or even longer time [Figure 4F], which has a high risk of causing suffocation. It is noted that the shape of the waveforms by the lying down-sitting up cycle and the snoring cycle seems similar, but the height and length are different due to varying sensing mechanisms. The waveform of lying down comes from the head hitting on the airbag

pillow with a high pressure, and thus has a high height (~1.0 relative current change). Its length depends on when the person sits up. The waveform of snoring comes from the inhale action with a small pressure, and thus has a small height (~0.04-0.07 relative current change). Its length depends on the snoring time, which can range from 2 to 8 s. Therefore, abnormal snoring activity can be timely detected by the intelligent pillow, and a warning could be made to wake the sleeper for safety.

### **Application of sensor array on airbag pillow for head posture recognition**

Monitoring the sleeping posture changes is of great significance for evaluating sleep quality, and the head posture is one of the important indicators to judge the health status during sleep. Although there are many sleep monitoring devices on the market to collect body movement information, most of them are wearable electronics that need to be tightly worn on the body and thus inevitably hinder the quiet sleeping experience. To overcome this practical limitation, herein we develop an intelligent pillow equipped with the developed five flexible and breathable sensors, which can detect and recognize the head posture with the help of the one-dimensional (1D) convolutional neural networks (CNNs) algorithm prediction model [Figure 5A]. The five sensors are aligned along the length direction on the surface of the pillow and labeled as A to E to distinguish different signal sources. Three head positions are set, including lying on the back, lying on the right side, and lying on the left side of the body. When the head comes into contact with the sensors at different positions during its flipping process, each sensor will individually output a corresponding real-time response signal upon its contacting state with the head. A multi-channel signal acquisition system is explored to simultaneously acquire the five sensors' output signals in a real-time mode, and the collected five-channel data information is fed into the built-in machine learning model for training (see detailed information on architecture, hyperparameters and sample sets in Supporting Information). Through one convolutional layer to extract the local features of the waveforms and one pooling layer to reduce the dimensionality of the data, a CNN prediction model is built after training and calibration. Then future testing data can be input into the trained model to obtain the prediction results.

In practice, volunteers are asked to lie down with heads on the pillow and perform the three different head positions so that characteristic waveforms obtained by the five sensors are collected [Figure 5B]. Totally 350 sets of data are obtained and randomly classified into three groups according to a ratio of 5:1:1. Among them, 250 sample data are used for the training set, 50 sample data are used in the testing set, and 50 sample data are used in the validation set. The gesture data sets show obvious differences after training [Figure 5C]. The 300-sample data including the training and test sets are input into the CNN framework for model training, yielding a high recognition rate for the three different head positions (Figure 5D; the confusion matrix shows the training results with an average accuracy of up to 98%).

## **CONCLUSIONS**

In summary, a flexible and breathable pressure sensor is developed on an all-paper platform. The sensor adopts a planar device structure with one MXene/dust-free paper as the piezoresistive layer on top of one dust-free paper with printed interdigital silver electrodes. SEM characterization confirms the achievement of the MXene-coating fabric network and the multilayered device structure. Measurements show that the sensor not only possesses good flexibility, air/moisture permeability, and wearing biocompatibility but also exhibits excellent sensing performance with a high sensitivity of  $16.7 \text{ kPa}^{-1}$ , a wide detection range of 100 kPa, fast response time of 50 ms and good stability over 10,000 cycles. Towards practical sensing applications for sleep monitoring, the single sensor unit is integrated into the airbag pillow for detecting snoring with different modes, and the five-sensor array is aligned for recognizing sleeping head posture with machine learning. The proposed paper-based sensor, along with the intelligent airbag pillow, provides a promising approach for sleep monitoring in a comfortable unrestricted way.

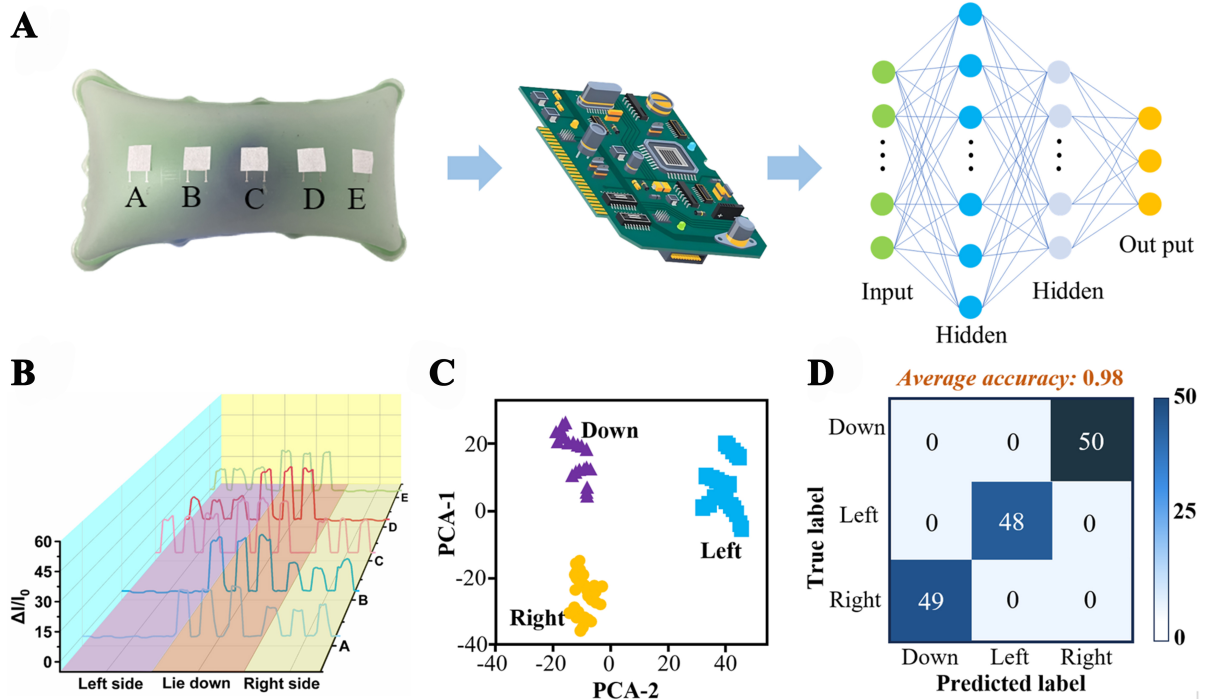


**Figure 5.** Integration of sensor array on airbag pillow for head posture recognition. (A) Schematic diagram illustrating the head posture recognition process through multi-channel sensing information acquisition by the pillow equipped with five sensors and machine learning by 1D CNN prediction model; (B) Different combinations of characteristic waveforms obtained by the five sensors for the three head postures; (C) Mapping of trained data in the 2D feature space; (D) Confusion matrix of the head gesture recognition classification results. 1D: One-dimensional; CNN: convolutional neural network; 2D: two-dimensional.

## DECLARATIONS

### Authors' contributions

Methodology, formal analysis, investigation, data curation, visualization, and writing - original draft: Zhang, Y.; Zhang, B.; Lv, Y.

Conceptualization, supervision, project administration, writing - review and editing: Wang, P.; Liu, T.; Meng, C.

### Availability of data and materials

The data presented in this study is available upon request from the corresponding author.

### Financial support and sponsorship

This work was supported by the China National Key Research and Development Program (No. 2022YFC3601400), and partially by the Tianjin Science and Technology Plan Project (No. 22JCZDJC00630) and the Higher Education Institution Science and Technology Research Project of Hebei Province (No. JZX2024024).

### Conflicts of interest

All authors declared that there are no conflicts of interest.

### Ethical approval and consent to participate

Not applicable.

## Consent for publication

Not applicable.

## Copyright

© The Author(s) 2025.

## REFERENCES

1. Jiang, Z.; Lee, Y. S.; Wang, Y.; John, H.; Fang, L.; Tang, Y. Advancements in flexible sensors for monitoring body movements during sleep: a review. *Sensors* **2024**, *24*, 5091. DOI PubMed PMC
2. Yuxin, P.; Li, S.; Xia, Z.; et al. Recent advances in flexible bending sensors and their applications. *Int. J. Smart. Nano. Mat.* **2024**, *15*, 697-729. DOI
3. Sun, G.; Wang, P.; Jiang, Y.; Sun, H.; Meng, C.; Guo, S. Recent advances in flexible and soft gel-based pressure sensors. *Soft. Sci.* **2022**, *2*, 17. DOI
4. Liu, Y.; Wang, H.; Zhao, W.; Zhang, M.; Qin, H.; Xie, Y. Flexible, stretchable sensors for wearable health monitoring: sensing mechanisms, materials, fabrication strategies and features. *Sensors* **2018**, *18*, 645. DOI PubMed PMC
5. Qi, J.; Yang, P.; Waraich, A.; Deng, Z.; Zhao, Y.; Yang, Y. Examining sensor-based physical activity recognition and monitoring for healthcare using Internet of Things: a systematic review. *J. Biomed. Inform.* **2018**, *87*, 138-53. DOI
6. Yang, Y.; Cui, T.; Li, D.; et al. Breathable electronic skins for daily physiological signal monitoring. *Nanomicro. Lett.* **2022**, *14*, 161. DOI PubMed PMC
7. Yuan, Z.; Han, S.; Gao, W.; Pan, C. Flexible and stretchable strategies for electronic skins: materials, structure, and integration. *ACS. Appl. Electron. Mater.* **2022**, *4*, 1-26. DOI
8. Zhang, L.; He, J.; Liao, Y.; et al. A self-protective, reproducible textile sensor with high performance towards human-machine interactions. *J. Mater. Chem. A.* **2019**, *7*, 26631-40. DOI
9. Cao, M.; Su, J.; Fan, S.; Qiu, H.; Su, D.; Li, L. Wearable piezoresistive pressure sensors based on 3D graphene. *Chem. Eng. J.* **2021**, *406*, 126777. DOI
10. Wang, H.; Li, Z.; Liu, Z.; et al. Flexible capacitive pressure sensors for wearable electronics. *J. Mater. Chem. C.* **2022**, *10*, 1594-605. DOI
11. Guo, X.; Li, Y.; Hong, W.; et al. Bamboo-inspired, environmental friendly PDMS/plant fiber composites-based capacitive flexible pressure sensors by origami for human-machine interaction. *ACS. Sustain. Chem. Eng.* **2024**, *12*, 4835-45. DOI
12. Tajitsu, Y. Piezoelectret sensor made from an electro-spun fluoropolymer and its use in a wristband for detecting heart-beat signals. *IEEE. Trans. Dielect. Electr. Insul.* **2015**, *22*, 1355-9. DOI
13. Li, H.; Wu, K.; Xu, Z.; Wang, Z.; Meng, Y.; Li, L. Ultrahigh-sensitivity piezoresistive pressure sensors for detection of tiny pressure. *ACS. Appl. Mater. Interfaces.* **2018**, *10*, 20826-34. DOI
14. Yang, J. C.; Kim, J. O.; Oh, J.; et al. Microstructured porous pyramid-based ultrahigh sensitive pressure sensor insensitive to strain and temperature. *ACS. Appl. Mater. Interfaces.* **2019**, *11*, 19472-80. DOI
15. Park, J.; Lee, Y.; Hong, J.; et al. Giant tunneling piezoresistance of composite elastomers with interlocked microdome arrays for ultrasensitive and multimodal electronic skins. *ACS. Nano.* **2014**, *8*, 4689-97. DOI
16. Tao, L. Q.; Zhang, K. N.; Tian, H.; et al. Graphene-paper pressure sensor for detecting human motions. *ACS. Nano.* **2017**, *11*, 8790-5. DOI
17. Wang, K.; He, Z.; Yu, Y. Preparation and performance optimization of flexible piezoresistive pressure sensor. *Electron. Comp. Mater.* **2022**, *41*, 781. DOI
18. Wang, P.; Liu, J.; Li, Y.; et al. Recent advances in wearable tactile sensors based on electrospun nanofiber platform. *Adv. Sens. Res.* **2023**, *2*, 2200047. DOI
19. Wang, P.; Yu, W.; Li, G.; Meng, C.; Guo, S. Printable, flexible, breathable and sweatproof bifunctional sensors based on an all-nanofiber platform for fully decoupled pressure-temperature sensing application. *Chem. Eng. J.* **2023**, *452*, 139174. DOI
20. Sun, G.; Wang, P.; Meng, C. Flexible and breathable iontronic tactile sensor with personal thermal management ability for a comfortable skin-attached sensing application. *Nano. Energy.* **2023**, *118*, 109006. DOI
21. Qin, R.; Nong, J.; Wang, K.; et al. Recent advances in flexible pressure sensors based on MXene materials. *Adv. Mater.* **2024**, *36*, e2312761. DOI
22. Shu, J.; Gao, L.; Li, Y.; et al. MXene/tissue paper composites for wearable pressure sensors and thermotherapy electronics. *Thin. Solid. Films.* **2022**, *743*, 139054. DOI
23. Chang, K.; Guo, M.; Pu, L.; et al. Wearable nanofibrous tactile sensors with fast response and wireless communication. *Chem. Eng. J.* **2023**, *451*, 138578. DOI
24. Shi, J.; Wang, L.; Dai, Z.; et al. Multiscale hierarchical design of a flexible piezoresistive pressure sensor with high sensitivity and wide linearity range. *Small* **2018**, *14*, e1800819. DOI
25. Wang, S.; Du, X.; Luo, Y.; et al. Hierarchical design of waterproof, highly sensitive, and wearable sensing electronics based on MXene-reinforced durable cotton fabrics. *Chem. Eng. J.* **2021**, *408*, 127363. DOI

26. Adepu, V.; Tathacharya, M.; Cs, R.; Mattela, V.; Sahatiya, P. TeNWs/Ti<sub>3</sub>C<sub>2</sub>T<sub>x</sub> nanohybrid-based flexible pressure sensors for personal safety applications using morse code. *ACS. Appl. Nano. Mater.* **2022**, *5*, 18209-19. DOI
27. Chen, Z.; Hu, Y.; Zhuo, H.; et al. Compressible, elastic, and pressure-sensitive carbon aerogels derived from 2D titanium carbide nanosheets and bacterial cellulose for wearable sensors. *Chem. Mater.* **2019**, *31*, 3301-12. DOI
28. Guo, Y.; Zhong, M.; Fang, Z.; Wan, P.; Yu, G. A wearable transient pressure sensor made with MXene nanosheets for sensitive broad-range human-machine interfacing. *Nano. Lett.* **2019**, *19*, 1143-50. DOI
29. Li, T.; Chen, L.; Yang, X.; et al. A flexible pressure sensor based on an MXene–textile network structure. *J. Mater. Chem. C.* **2019**, *7*, 1022-7. DOI
30. Liu, R.; Li, J.; Li, M.; et al. MXene-coated air-permeable pressure-sensing fabric for smart wear. *ACS. Appl. Mater. Interfaces.* **2020**, *12*, 46446-54. DOI
31. Lu, Y.; Qu, X.; Zhao, W.; et al. Highly stretchable, elastic, and sensitive MXene-based hydrogel for flexible strain and pressure sensors. *Research* **2020**, *2020*, 2038560. DOI PubMed PMC
32. Zheng, Y.; Yin, R.; Zhao, Y.; et al. Conductive MXene/cotton fabric based pressure sensor with both high sensitivity and wide sensing range for human motion detection and E-skin. *Chem. Eng. J.* **2021**, *420*, 127720. DOI